FEBS Open Bio 4 (2014) 251–259

journal homepage: www.elsevier.com/locate/febsopenbio

The DNA intercalators ethidium bromide and propidium iodide also bind to core histones

Amrita Banerjee [a], Parijat Majumder [a,1], Sulagna Sanyal [a], Jasdeep Singh [a,2], Kuladip Jana [b], Chandrima Das [a,*], Dipak Dasgupta [a,*]

[a] Biophysics & Structural Genomics Division, Saha Institute of Nuclear Physics, Block-AF, Sector-1, Bidhan Nagar, Kolkata 700064, West Bengal, India
[b] Division of Molecular Medicine, Centre for Translational Animal Research, Bose Institute, P-1/12 C.I.T. Scheme VIIM, Kolkata 700054, West Bengal, India

ARTICLE INFO

Article history:
Received 9 September 2013
Revised 11 February 2014
Accepted 11 February 2014

Keywords:
Chromatin compaction
Histone and DNA binding
DNA release
Histone acetylation

ABSTRACT

Eukaryotic DNA is compacted in the form of chromatin, in a complex with histones and other non-histone proteins. The intimate association of DNA and histones in chromatin raises the possibility that DNA-interactive small molecules may bind to chromatin-associated proteins such as histones. Employing biophysical and biochemical techniques we have characterized the interaction of a classical intercalator, ethidium bromide (EB) and its structural analogue propidium iodide (PI) with hierarchical genomic components: long chromatin, chromatosome, core octamer and chromosomal DNA. Our studies show that EB and PI affect both chromatin structure and function, inducing chromatin compaction and disruption of the integrity of the chromatosome. Calorimetric studies and fluorescence measurements of the ligands demonstrated and characterized the association of these ligands with core histones and the intact octamer in absence of DNA. The ligands affect acetylation of histone H3 at lysine 9 and acetylation of histone H4 at lysine 5 and lysine 8 *ex vivo*. PI alters the post-translational modifications to a greater extent than EB. This is the first report showing the dual binding (chromosomal DNA and core histones) property of a classical intercalator, EB, and its longer analogue, PI, in the context of chromatin.

1. Introduction

In a eukaryotic cell, DNA is a component of chromatin, where it exists in complex with histones and non-histone proteins. Therefore, DNA serves not only as a repository of encoded sequence information, but also as a scaffold on which DNA binding proteins assemble. Nucleosome is the basic repeating unit of chromatin [1–3] which is composed of 145–147 bp of DNA, wrapped around an octamer of histone proteins in 1.65 turns of a left-handed superhelix.

The intimate association of proteins and DNA raises the possibility that a DNA-interactive small molecule may interfere with processes that are associated with the protein assemblies [4]. Likewise, the DNA-binding compounds may bind to chromatin associated proteins as well. There is a dearth of reports which study the ability of the classical DNA intercalators to bind core histones in absence of DNA scaffold.

Histone post-translational modification as well as DNA methylation can be impacted by these small molecule modulators. In this context, we earlier proposed a classification of DNA-binding ligands in two types: single binding mode and dual binding mode in the chromatin context [5,6]. The former class of ligands binds to chromosomal DNA only while the later has the ability to bind both histone(s) and chromosomal DNA. Studies from our laboratory and others had shown that the plant alkaloid sanguinarine [7], daunomycin and mitoxantrone [8,9] interact with both DNA and core histones and affect post-translational modifications like histone acetylation [10].

With the above broad objective, we have investigated the chromatin binding properties of a classical DNA intercalator, ethidium bromide and its structural longer analogue, propidium iodide

Abbreviations: EB, ethidium bromide; PI, propidium iodide; ITC, isothermal titration calorimetry; DLS, dynamic light scattering; HMG, high mobility group; Oct, octamer; HAT, histone acetyl transferase; MTT, (3-(4-5 dimethylthiozol-2-yl) 2-5diphenyl-tetrazolium bromide)

* Corresponding authors. Tel.: +91 33 23375345x3506; fax: +91 33 2337 4637.
E-mail addresses: chandrima.das@saha.ac.in (C. Das), dipak.dasgupta@saha.ac.in (D. Dasgupta).
[1] Present address: Department of Molecular Structural Biology, Max Planck Institute of Biochemistry, Am Klopferspitz 18, 82152 Martinsried, Germany.
[2] Present address: Kusuma School of Biological Sciences, Indian Institute of Technology-Delhi, HauzKhas, New Delhi 110016, India.

http://dx.doi.org/10.1016/j.fob.2014.02.006
2211-5463/

(henceforth abbreviated as EB and PI, respectively; Fig. 1) [11,12] at different levels of chromatin. Both ligands contain identical aromatic phenanthridinium planar rings. The difference is the presence of a linear side chain containing quaternary amine group in PI. It makes the molecule doubly charged. Binding of these cationic molecules reduce the effective charge density of DNA. These phenanthrene derivatives lengthen and unwind the DNA double helix [13,14] and introduce a tilt between adjacent base pairs [15]. Binding of one molecule of EB unwinds the DNA helix by an angle of 26° [13,14]. As a result, it affects the torsional and bending flexibilities of DNA. PI exhibits similar binding properties. These molecules have been widely used to probe various configurations of DNA [16–30].

Earlier reports had shown that, EB derivatives bind preferentially to the linker segment compared to the nucleosome in the extended chromatin fiber [31–33]. In compact chromatin, EB promotes the release of histone H1 and thus has the potential to disrupt higher order chromatin structures [25]. Consequently, EB and other intercalating agents had been used to investigate the motional dynamics of nucleosome core particle [34,35], to analyze nucleosome phasing in active genes [36] and to identify torsional stress in genomes [37,38]. Reports of the interaction of PI with chromatin are relatively few [39,40]. However, it is known that both EB and PI induce specific release of the high mobility group (HMG) proteins, HMG 14, HMG 17 and other DNA-binding proteins from chicken erythrocyte chromatin [41].

Current report focuses on studying the effect of the above classical intercalators, EB and PI (Fig. 1), on chromatin structure and the effect upon the core histone-DNA assembly. Though there are a large number of reports for these widely used ligands, there is a lacuna *vis-à-vis* the knowledge of their interactions with histone proteins in chromatin. By means of steady state fluorescence spectroscopy and isothermal titration calorimetry (ITC), we have made a quantitative evaluation of the binding parameters for the association of EB and PI with soluble chromatin and its components, namely, chromatosomes, chromosomal DNA and most importantly the core histones. In addition we have monitored the effect of the intercalators on chromatin structure by means of dynamic light scattering and chromatosome stability assay. We find that EB and PI interact with both DNA and histone components of chromatin to cause compaction. As a sequel to our demonstration of the association of core histones with the intercalators, we have shown that both the intercalators affect histone H3 and H4 acetylations *in vitro* and *ex vivo*. Such in-depth study of the association of these

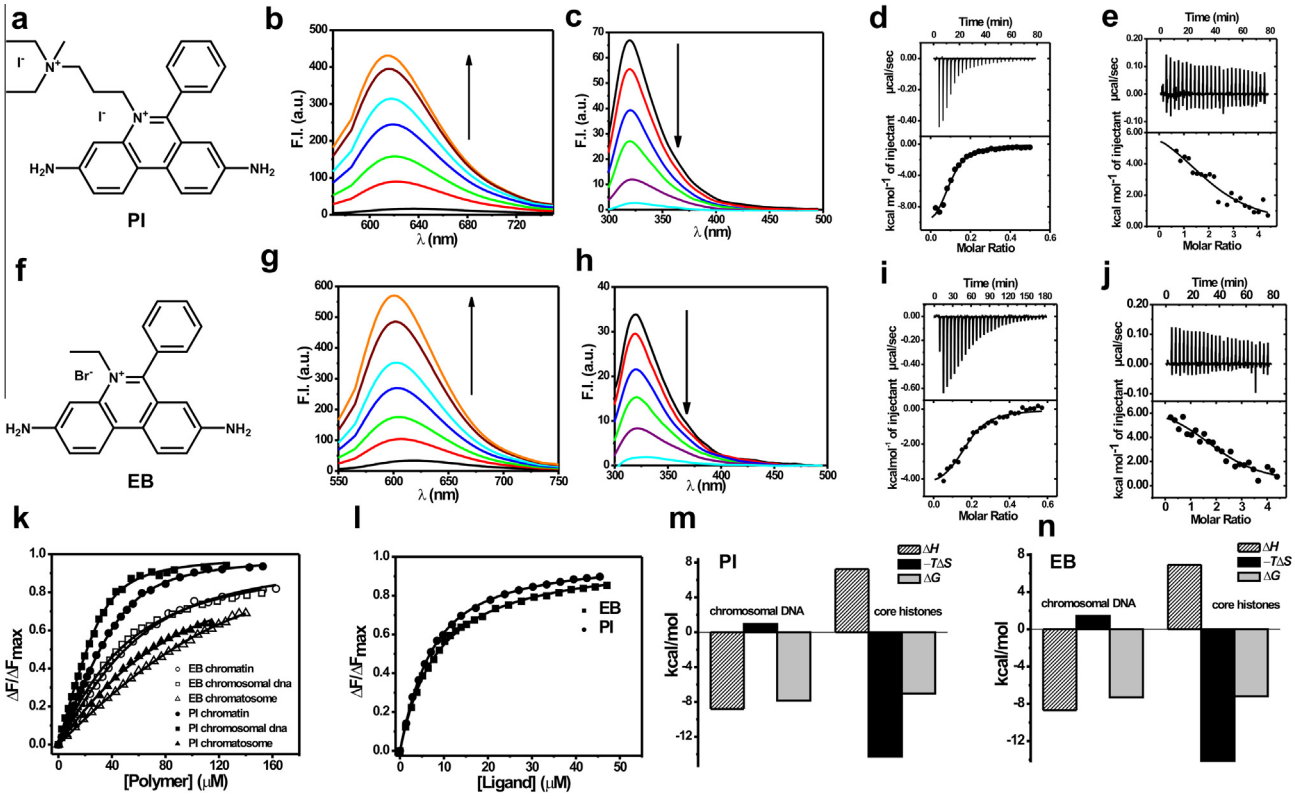

Fig. 1. Association of propidium iodide and ethidium bromide with hierarchical levels of chromatin and core histones monitored by steady state fluorescence spectroscopy and isothermal titration calorimetry: (a) Chemical structure of propidium iodide (PI). (b) Emission spectra of PI in absence (black) and presence of increasing concentrations (9.5, 19, 33, 47, 82, and 143 μM) of long chromatin. λ_{ex} = 536 nm. (c) Emission spectra of core histone octamer in absence (black) and presence of increasing concentrations (1.5, 4.2, 8.4, 17.2, and 40 μM) of PI. λ_{ex} = 278 nm. (d) ITC profile for the association of PI with long chromatin. (e) ITC profile for the association of PI with core histones. (f) Chemical structure of ethidium bromide (EB). (g) Emission spectra of EB in absence (black) and presence of increasing concentrations (9.5, 19, 33, 47, 82, and 143 μM) of long chromatin. λ_{ex} = 520 nm. (h) Emission spectra of core histone octamer in absence (black) and presence of increasing concentrations (1.5, 4.2, 8.4, 17.2, and 40 μM) of EB. λ_{ex} = 278 nm. (i) ITC profile for the association of EB with long chromatin. (j) ITC profile for the association of EB with core histones. (k) Binding isotherms for the interaction of PI and EB with hierarchical levels of chromatin obtained from steady state fluorescence spectroscopy. Data points for long chromatin, chromatosome and chromosomal DNA are denoted by circles, triangles and squares respectively. The experimental set for PI shows black fills and the set with no fill shapes correspond to EB. The concentration of PI/EB was taken 3 μM in these fluorimetric titrations. (l) Binding isotherms for the interaction of histone octamer [1.5 μM] with PI (circles) and EB (squares) as obtained from steady state fluorescence spectroscopy. (m) Binding energetics of the interaction of PI with chromosomal DNA (left) and core histones (right). (n) Binding energetics of the interaction of EB with chromosomal DNA (left) and core histones (right). The enthalpy change for the ligand-macromolecule association is denoted by ΔH, the entropy factor is denoted by $T\Delta S$ and the free energy change for the interaction is denoted by ΔG in each case in (m) and (n). The upper panels in the ITC profiles in (d, e, i and j) show the heat of association for ligand-macromolecule interactions. The lower panels show the heat exchanged per mole of injectant as a function of molar ratio of ligand to macromolecule. The solid lines represent the fitted isotherms obtained using "one set of sites" binding model. The thermograms have been fitted after subtracting appropriate controls. The heat changes for the controls are shown in the supplementary section. All the experiments in Fig. 1 were performed at 25 °C.

ligands with chromatin at different levels and demonstration of the outcome of the association has not been reported till date. The broad objective of our study is to classify small DNA binding molecules in terms of their ability to bind chromosomal DNA alone and/or both histones and chromosomal DNA (dual binding mode) [5–7,42]. The results presented here show the core histone binding ability of a classical intercalator and its structural analogue.

2. Materials and methods

2.1. Materials

Chemicals were purchased from Sigma Chemical Company, USA and used without further purification. Histone acetyltransferase GCN5 (Catalogue No. BML-SE272) was from Enzo Life Sciences. H3K9Ac (Catalogue No. 07-352, Millipore), H4K5Ac (Catalogue No. ab61236, Abcam), H4K8Ac (Catalogue No. ab15823, Abcam), H3K14Ac (Catalogue No. 07-353, Millipore), H3 (Catalogue No. ab1791, Abcam), H4 (Catalogue No. ab10158, Abcam) and β-Actin (Catalogue No. W402B, Promega) primary antibodies have been used. Chemiluminescent substrates were from Thermo Scientific (SuperSignal West Pico Substrate).

2.2. Methods

2.2.1. Preparation of EB and PI solutions

Concentrated stock solutions were prepared in experimental buffer and the concentrations were determined in water, spectrophotometrically, using the molar extinction coefficients of 5600 M^{-1} cm^{-1} at 480 nm for EB [43] and 5950 M^{-1} cm^{-1} at 493 nm for PI [44].

2.2.2. Preparation of chromatin samples

Chromatin and chromatosome were isolated from HeLa cells as per standard protocol [45]. Briefly, HeLa nuclear pellet was digested with MNase (0.2 Units/μL) followed by extraction in TE buffer. Sucrose gradient fractionation (5–25%) was carried out to purify chromatosome from longer chromatin fragments.

Chromatin and chromatosomes from Sprague–Dawley rat livers were isolated using the method detailed elsewhere [42,46]. Partial Micrococcal Nuclease digestion of chromatin was performed (1 μL from 50 Units/μL MNase stock added to 400 μL digestion mixture). The solubilized chromatin was purified by ultracentrifugation through a 5–25% linear sucrose density gradient and long fragments and chromatosomes were separately collected.

Chromosomal DNA was isolated from soluble chromatin by phenol – chloroform – isoamyl alcohol extraction followed by precipitation with isopropanol. The integrity of chromatin, chromatosome and chromosomal DNA, was checked by agarose gel electrophoresis (Fig. S1). All samples, prior to experiment were dialyzed extensively against 50 mM Tris–HCl (pH 8.0) and mononucleotide concentrations of the samples were determined spectrophotometrically using the molar extinction coefficient (ε_{260}) of 6600 M^{-1} cm^{-1}.

2.2.3. Purification of HeLa core histones

Core histones were prepared from HeLa nuclear pellet following the standard protocol [47]. Purity checked on SDS PAGE.

2.2.4. Isothermal titration calorimetry

Chromatin, chromatosome and chromosomal DNA were titrated against EB and PI in 50 mM Tris–HCl (pH 8.0). Titrations with EB were carried out in a MicroCal VP-ITC microcalorimeter. Typically, 1.4 ml of macromolecule (90–150 μM DNA base), loaded in the calorimetric cell was titrated against 1-1.5 mM of EB solution using a 289 μL syringe, rotating at 286 rpm. Enthalpy changes due to EB dilution in buffer served as control. Titrations with PI were carried out in a MicroCal ITC 200 microcalorimeter. Typically, 200 μL of macromolecule (150–200 μM DNA base), loaded in the calorimetric cell was titrated against 350–500 μM of PI solution using a 40 μL syringe, rotating at 300 rpm. ITC measurements of PI dilution in buffer served as control.

Ligand interactions with core histones were studied in a MicroCal ITC 200 microcalorimeter. For ITC experiments, 9.5 μM of core histones (diluted in the dialysate containing 150 mM NaCl) was loaded in a 200 μL calorimetric cell. It was titrated against 200 μM EB or similar concentration of PI contained in a 40 μL syringe. The reaction was performed at 25 °C under constant stirring at 300 rpm. Control experiments were performed by titrating EB or PI against the histone dialysate. Buffer from syringe was also added to 9.5 μM of core histones, which served as another control. Based on the Levenberg–Marquardt non-linear least squares curve fitting algorithm, the resulting thermograms were analyzed using one set of binding sites model of the MicroCal LLC software.

2.2.5. Dynamic light scattering

The effects of EB and PI on the hydrodynamic size of chromatin and histone octamer were monitored by DLS. The measurements were performed on a Zetasizer Nano S particle analyzer from Malvern Instruments, UK, whereby a He–Ne laser (633 nm) utilizing 4 mW power at 632.8 nm is used as the light source. The intensity autocorrelation function generates a correlation curve. Cumulants analysis of the correlation curve gives the intensity weighted mean hydrodynamic diameter or Z_{av} diameter of the sample.

In order to study the effect of EB and PI on the hydrodynamic size of soluble chromatin, the sample (400 μM mononucleotides) was treated with EB and PI in drug to DNA base ratio of 0, 0.05, 0.10, 0.15 and 0.20 at 25 °C and the same were monitored by DLS.

To study the effect of EB and PI on the hydrodynamic diameter of histone octamer, 5 μM of histone octamer was treated with EB and PI in EB/PI to octamer ratios of 0, 0.5, 1.0, 2.0, 3.0, 6.0, and 12.0. The corresponding hydrodynamic diameters were then analyzed with respect to their number percentages by DLS.

2.2.6. Steady state fluorescence measurements

The fluorescence measurements were performed in a Perkin Elmer LS 55 Luminescence Spectrometer at 25 °C. The fluorescence emission spectra of PI and EB were monitored in presence of chromatin, chromatosome, chromosomal DNA and core histone octamer. The samples were excited at 536 nm in case of PI and 520 nm in case of EB. The fluorescence anisotropy values were evaluated from fluorescence intensity values at the respective emission maximum. The excitation and emission slit widths were adjusted to 10 nm and each spectrum was an average of 4 scans with a scan speed of 200 nm/min. The incubation time after the addition of each aliquot was 3 min. The emission spectrum of core histones was also monitored in presence of PI and EB to determine the dissociation constants of ligand–histone interactions. In this case the samples were excited at 278 nm, other parameters were kept unchanged. Binding analyses of fluorimetric titrations were done using standard non-linear curve fitting method [48,49]. Binding stoichiometry was determined from the intersection of two straight lines obtained from the least-squares fit plot of normalized change in fluorescence against the input concentration of the titrant.

2.2.7. Circular dichroism study

The circular dichroism measurements were performed in a Spectropolarimeter from Bio Logic Science Instruments, France and data were analysed with inbuilt Bio-Kine 32 V4.49-1 software.

3 μM histone octamer was titrated against increasing concentrations of EB (0, 1.5, 3, 6, 9, 18 and 36 μM) at 25 °C. The molar ellipticity was plotted against the wavelength. Acquisition duration was fixed at 2 s and a wavelength range of 200–275 nm was scanned at 0.5 nm intervals. Each spectrum was an average of 4 accumulations and the corrected spectra were obtained by subtraction of respective control. The control experiment was performed keeping everything same excluding the octamer and using dialysate instead.

2.2.8. Chromatosome stability assay

Chromatosomes were incubated with EB and PI in drug to DNA base ratio of 0, 0.05, 0.10, 0.15 and 0.20 for 30 min at 37 °C. The samples were then analyzed by electrophoresis on 1.5% agarose gel in 0.5× TBE, followed by staining with SYBR green.

2.2.9. Histone acetyltransferase (HAT) assay

HAT assay was performed as per standard protocol [47]. 2 μg of HeLa core histone protein was incubated in HAT assay buffer (50 mM Tris–HCl, pH 8.0, 10% (v/v) glycerol, 1 mM dithiothreitol, 1 mM phenylmethylsulfonyl fluoride, 0.1 mM EDTA pH 8.0 and 0.1 mM sodium butyrate) in presence and absence of EB/PI at 30 °C for 10 min. The first incubation step was followed by the addition of 1 μL of acetyl-CoA and was further incubated for another 10 min at 30 °C. The acetylation reaction was terminated by chilling on ice. Core histone was precipitated by trichloroacetic acid (TCA) precipitation and analyzed on a 15% SDS page followed by western blot analysis. Anti-H3K9Ac antibody was used at 1:10,000 dilutions.

2.2.10. Cell culture and treatment with the ligands

HeLa cells were maintained in Dulbecco's modified Eagle's medium (Gibco) supplemented with 10% fetal bovine serum (Gibco) and penstrep (10 μL/mL of medium from a stock of penicillin (10000 Units/mL) and streptomycin (10000 μg/mL), Gibco) at 37 °C. The cells were treated with different concentrations of PI and EB for 3 h and processed for immunoblot analysis. H3K9Ac (dilution 1:10000), H3K14Ac (dilution 1:5000), H4K5Ac (dilution 1:1000) and H4K8Ac (dilution 1:1000) acetylation marks were probed.

2.2.11. Cell viability assay (MTT assay)

Inorder to check cell viability on ligand treatment, MTT assay was performed as per standard protocol [50]. Briefly, HeLa cells were treated with different concentrations of ligands (2, 4, and 8 μM) for 3 h, followed by MTT (3-(4-5 dimethylthiozol-2-yl) 2-5diphenyl-tetrazolium bromide) treatment (100 μg/μL) for 4 h at 37 °C. Absorbance measurements were taken in a UV–visible spectrophotometer (Cecil 7500) at 570 nm. Background subtraction was performed at 650 nm. Percent cell viability was plotted for each set (untreated and treated). $O.D._{570}$–$O.D._{650}$ for the control set corresponds to 100% viable cells.

3. Results

3.1. Characterization of ligand–chromatin interaction at different hierarchical levels of chromatin and the associated thermodynamics

Steady state fluorescence spectroscopy has been used to determine the binding affinity and binding stoichiometry of the ligands with chromatin components obtained from HeLa cells. Association of chromatin, chromatosome and chromosomal DNA (subsequently denoted as polymers) with PI/EB is characterized by blue shift of the emission maximum of PI and EB with a concomitant increase in fluorescence quantum yield (Fig. 1, panels, b and g). The resultant binding isotherms are shown in Fig. 1, panel k. The apparent dissociation constants determined using nonlinear curve fitting analysis [48,49] and the binding stoichiometry are summarized in Table 1. The ligands show maximum affinity for chromosomal DNA. The trend of the dissociation constants at 25 °C follows the order; K_d (chromatosome) > K_d (chromatin) > K_d (chromosomal DNA). Isothermal titration calorimetry has been employed in case of rat liver chromatin and its components to evaluate the binding energetics. The trend in dissociation constant follows the same order as reported above for HeLa cell. It implies that the interaction of the ligands with chromatin assembly is not system specific. The disparity in the dissociation constant values between fluorescence and calorimetry could be attributed to the principles of the two techniques. Such variation in magnitude of the binding affinities obtained from the two methodologies is not counter-intuitive and was reported earlier in case of polymer-small ligand association [51]. Representative thermograms for titrations of rat liver chromatin with PI and EB at 25 °C are shown in Fig. 1. In control experiments the enthalpy changes due to dilution of the ligands in the buffer (Supplementary Fig. S2) has been carried out and appropriately subtracted to get the final thermograms. The results obtained from such thermograms are summarized in Table 2. The observations from Fig. 1 and the results from Tables 1 and 2, could be summed up as follows. Both ligands bind to chromatin, chromatosome and chromosomal DNA with micromolar dissociation constants. The affinity constant, binding stoichiometry and enthalpy of EB-chromatin/chromosomal DNA interactions are comparable with earlier reports [31]. Previously, calorimetric approaches were applied to characterize Hoechst–DNA interaction [51,52], and ethidium/propidium–DNA association [39]. The range of enthalpy values is comparable to our current data. Similar parameters were reported from our laboratory for the association of the classical groove binder, distamycin, with chromatin and its components from the same source [42]. The association is found to be enthalpy driven. However, the higher magnitudes of favorable negative enthalpy contributions make the association tighter in this case. Notably, previous report suggested that binding of 14 EB molecules to each nucleosome core particle is necessary to initiate dissociation of the core particle [53] and have efficiently demonstrated the extent of differential external electrostatic and internal intercalation binding modes of EB [54]. In case of association with chromatosome, EB has a notably lower affinity in comparison to chromatin. It might originate from the absence of linker DNA in chromatosome. PI, in general, interacts with chromatin and its components with higher affinity than EB. This is because the doubly charged intercalator, PI, binds to naked DNA with a higher affinity than EB [55]. The higher binding stoichiometry in case of PI can be ascribed to the presence of a longer chain in the non-aromatic moiety. As expected, all associations are enthalpy driven suggesting important role of electrostatic

Table 1
Apparent dissociation constants and binding stoichiometry obtained from steady state fluorescence spectroscopy at 25 °C.

Ligand	Polymer	K_d (μM)	Stoichiometry (n)
PI	Chromatin	30.9 ± 0.4	17.8[a]
	Chromatosome	69.0 ± 0.9	20.0[a]
	Chromosomal DNA	21.0 ± 0.5	12.3[a]
	Core histone octamer	5.9 ± 0.2	6.2[b]
EB	Chromatin	50.2 ± 0.5	20.9[a]
	Chromatosome	84.4 ± 1.0	22.1[a]
	Chromosomal DNA	44.2 ± 0.6	17.1[a]
	Core histone octamer	7.7 ± 0.1	5.7[b]

[a] n = DNA bases/ligand.
[b] n = ligand/histone octamer.

Table 2
Thermodynamic parameters obtained from ITC at 25 °C.

Ligand	Polymer	K_d (μM)	Stoichiometry (n)	ΔH (kcal mol^{-1})	ΔS (e.u.)	ΔG (kcal mol^{-1})
PI	Chromatin	3.7 ± 0.06	10.2[a]	−11.7 ± 0.9	−14.9	−7.26
	Chromatosome	5.6 ± 0.2	14.0[a]	−7.9 ± 0.6	−2.2	−7.24
	Chromosomal DNA	1.8 ± 0.04	8.3[a]	−8.8 ± 0.5	−3.2	−7.85
	Core histone assembly	7.0 ± 0.3	2.2[b]	7.3 ± 1.9	47.9	−7.0
EB	Chromatin	8.3 ± 0.4	5.0[a]	−7.9 ± 0.8	−4.8	−6.5
	Chromatosome	15.6 ± 0.7	6.7[a]	−5.6 ± 0.6	3.21	−6.6
	Chromosomal DNA	5.2 ± 0.06	4.8[a]	−8.7 ± 0.3	−4.8	−7.3
	Core histone assembly	5.2 ± 0.2	2.3[b]	6.9 ± 0.8	47.4	−7.2

[a] n = DNA bases/ligand.
[b] n = ligand/core histone assembly.

and other non-covalent association like hydrogen bonding and stacking interactions. Another notable finding is that presence of histones does not adversely affect the binding stoichiometry. It implies that accessibility to the DNA wrapping the core histones is not reduced. Alternately this may also arise from the binding potential of the two ligands with histones as has been subsequently validated.

3.2. Hydrodynamic characterization of small molecule–chromatin interaction

As a sequel to thermodynamic characterization of the association of the ligands with chromatin, we examined their effects upon the size of chromatin. Keeping in mind the fact that dynamic light scattering (DLS) measurements might give a clue to alteration in apparent size of a solvated dynamic particle, we have used DLS experiments, because in chromatin, a multimer of nucleosomes, the extent of structural changes would be more apparent. Our results as shown in Fig. 2 show that EB and PI interact with chromatin leading to compaction of chromatin. Fig. 2 illustrates the intensity statistics of 10 measurements each for chromatin and the same in presence of increasing concentrations of PI (Fig. 2a) and EB (Fig. 2b). With increasing concentrations of ligand, there is a significant change in the nature of the intensity histogram. Chromatin in absence of PI or EB shows two peaks, maximizing at 164.2 and 18.7 nm, respectively. At an EB to DNA base ratio of 0.05, although two peaks remain at similar positions, but the peaks tend to merge. At higher input ratios, a single peak is observed, that maximizes at 91.28 nm. In presence of PI, a single peak is observed at and above PI/DNA input ratio of 0.05. However, the peak shifts from 122.4 nm (at [PI]/[DNA] = 0.05) to 105.7 nm (at [PI]/[DNA] = 0.15) and again regains the value of 164.2 nm at [PI]/[DNA] = 0.2. For EB, the reduction in values of the mean intensity peak and Z_{av} diameter clearly indicates chromatin compaction. The extent of compaction is less in case of PI. Another important observation is the gradual decrease in polydispersity index, with

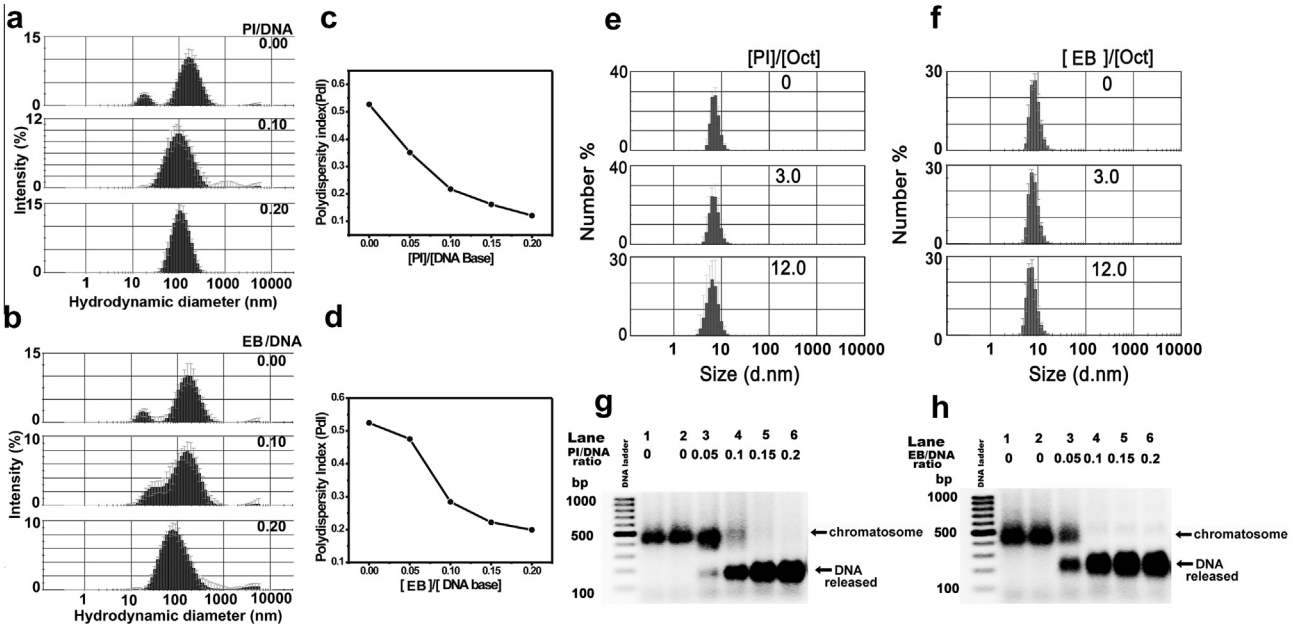

Fig. 2. Effect of the ligands on the structure of chromatin and its components monitored by dynamic light scattering (DLS) and agarose gel electrophoresis: Panels (a–f) depict the results obtained from DLS employed to study the influence of PI and EB on the hydrodynamic size of chromatin and histone octamer at 25 °C: Intensity statistics of 10 measurements are plotted for chromatin (400 μM DNA base) in presence of increasing concentrations of PI (a) and EB (b). The corresponding polydispersity index is plotted against input ratio of PI (c) and EB (d). The number statistics of 10 measurements each are plotted for 5 μM histone octamer (Oct) in presence of increasing concentrations of PI (e) and EB (f). Error bars indicate standard deviations. Panels (g) and (h) show the results of chromatosome stability assay performed to study the effect of PI and EB on chromatosome: Chromatosome samples (400 μM DNA base) were incubated with PI (g) and EB (h) at 37 °C for 30 min at ligand/DNA base ratio indicated, post-stained with Sybr green and analyzed on 1.5% agarose gel. Fresh chromatosome sample (lane 1) and chromatosome incubated with buffer at 37 °C for 30 min (lane 2) serve as negative controls in each case. The bands around 500 bp correspond to intact chromatosome and the bands around 200 bp correspond to the DNA released from the chromatosome as a result of incubation with the ligands. The 100 bp DNA ladder has been used as the marker.

increasing input ratios to DNA of EB and PI (Fig. 2c and d). Decrease in polydispersity index implies that the system is tending towards homogeneity. Upon compaction, soluble chromatin acquires a hydrodynamically homogenous form, which is reflected in the reduced polydispersity index. Similar trend was reported earlier for the groove binder, distamycin, from our laboratory [42].

3.3. Ligand – induced destabilization of chromatin structure at chromatosome level

EB was reported to destabilize nucleosome [56]. We also noticed that both intercalators, EB and PI, have the potential to disrupt the integrity of histone-DNA complexes in chromatosome leading to the release of free DNA. Panels (g and h) of Fig. 2 show the electrophoretic analysis of the effect of EB and PI on chromatosomes. Both cause destabilization of the chromatosome structure at a ligand to DNA base ratio as low as 0.05. At this ratio, there is partial disruption of the chromatosome structure. At and above ligand to DNA base ratio of 0.1, there is complete disruption of the chromatosome structure. Presence of a single band, around 200 bp indicates the release of DNA from the chromatosome (~400 bp) that provides evidence for the above inference (Fig. 2).

3.4. EB and PI bind to core histones and alter histone H3 and H4 acetylation marks

The results obtained so far gave us the clue to check the association of the intercalators with core histones. We had earlier reported association of another intercalator, sanguinarine, with core histones and its effect upon the histone modification, acetylation potential [7]. ITC experiments provide direct evidence for the interaction of PI and EB with core histones at low ionic strength (Fig. 1 panels, e and j). The control enthalpy change in buffer due to dilution of each ligand is shown in Supplementary Fig. S3 and the control enthalpy change for buffer–histone interaction is shown in Supplementary Fig. S4. At 25 °C the dissociation constant for EB–histone interaction is 5.2 μM, whereas that for PI–histone interaction is 7 μM. Unlike the interaction with chromatin, binding of both ligands to histones is mainly entropy driven. The thermodynamic parameters are summarized in Table 2. Release of bound water as a result of the association is the plausible factor behind positive enthalpy change. The value of the dissociation constant is in the same range as ligand-DNA association. The major difference is the enthalpy-driven nature of the association in the case of DNA. The opposite nature of the thermodynamics of association with chromosomal DNA and core histones might be due to opposite nature of net charges of DNA and histone(s).

Earlier report had shown that at low ionic strength the following equilibria exist in the core histone assembly: octamer ↔ H2A–H2B heterodimers + $H3_2H4_2$ tetramers [57]. On the other hand, the formation of core histone octamer takes place at high ionic strength (2 M NaCl) in absence of any factor. Limitation in the solubility of the octamer stands in our effort to make a thermodynamic evaluation by ITC of the association of core octamer population alone with the ligands. Therefore, we resorted to three other methods to examine the association of the ligands with core histone octamer: fluorescence, CD spectroscopy and dynamic light scattering. Steady state fluorescence measurements suggest an interaction between histone octamer and the ligands (Fig. 1, panels, c and h). The fluorescence intensity at the emission maximum of histone octamer decreases gradually with addition of the ligands until it reaches saturation. The binding isotherms are depicted in Fig. 1, panel l. At 25 °C the dissociation constants for interaction of PI and EB with HeLa core histone octamer obtained from fluorimetric titrations are 5.9 and 7.7 μM respectively. The K_d values at 25 °C for the interaction of core histone assembly with

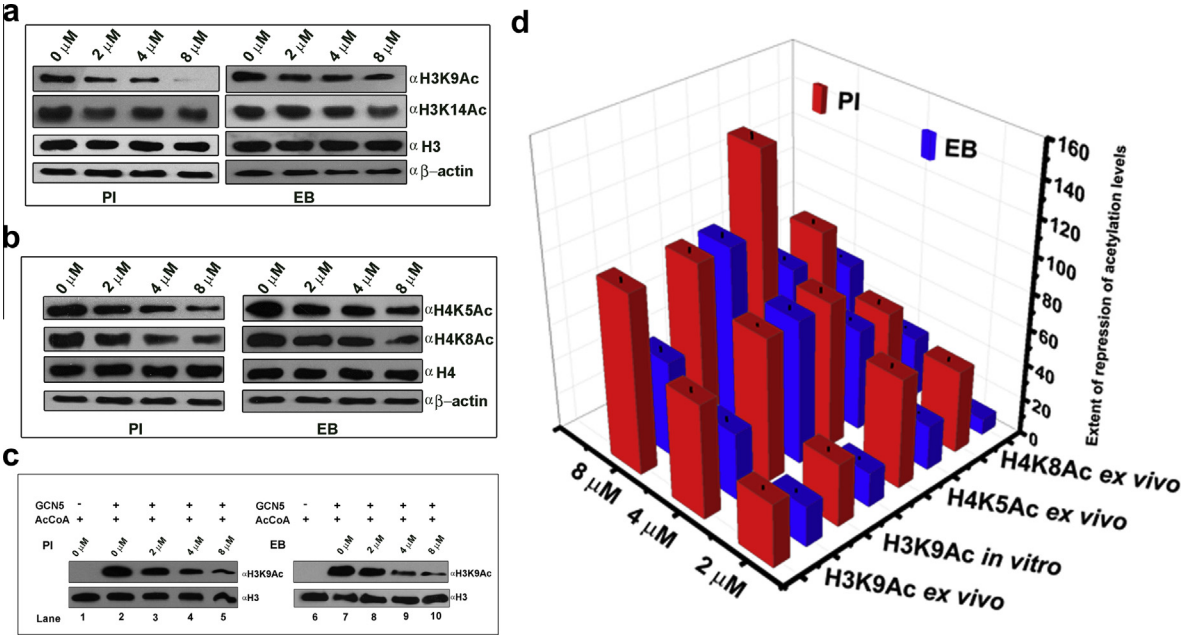

Fig. 3. Modulation of acetylation levels of histones H3 and H4 by the ligands (PI and EB) monitored by western blot analyses: (a) Effect of PI/EB on histone H3 acetylation at lysine 9 and 14 in HeLa cells. β-actin and histone H3 have been used as loading controls. (b) Ligand induced alteration of histone H4 acetylation at lysine 5 and 8 in HeLa cells. β-actin and histone H4 have been used as loading controls. (c) Histone acetyltransferase (HAT) assay performed in absence and presence of the ligands using purified HeLa core histones (2 μg) and processed for immunoblot analysis. No enzyme (lane 1 and 6) and no ligand (lanes 2 and 7) controls are shown. Alteration of histone H3K9Ac status in presence of increasing concentrations (2, 4, and 8 μM) of PI and EB are shown in lanes 3–5 and lanes 8–10, respectively. Loading and transfer of equal amounts of core histones were confirmed by immunodetection of histone H3. (d) Quantification of the extent of ligand induced hypoacetylations. The extent of repression of acetylation marks (H3K9Ac, H4K5Ac and H4K8Ac) in presence of the ligands has been quantified using Image J software and represented in the 3D plot against different concentrations of the ligands. The autoradiograms were quantified using Image J software after normalizing with respective histone H3 and H4 loading controls. Then the fold change was calculated in Origin. The error bars were estimated from three independent sets of experiments.

PI and EB at low and high ionic strengths estimated from two different histone sources are comparable. Fluorescence polarisation anisotropy values of free PI and EB also increase in presence of histone octamer suggesting association leading to complex formation. The FPA value of PI increased from 0.05 to 0.087 at a ligand/octamer ratio of 2.8 and the FPA value of EB increased from 0.02 to 0.066 at the same ligand/octamer ratio. Distribution of the hydrodynamic diameter of histone octamer with respect to its number percentage (Fig. 2e and f) or volume percentage (data not shown) does not change significantly even in presence of large excess of either ligand. Interestingly, the interaction of both ligands with histone octamer (i.e. in presence of 2 M NaCl) does not lead to dissociation of the octamer. It is noted that the mean diameter of ligand untreated chicken erythrocyte histone octamer is 8.12 nm, which agrees well with the value of 7.87 nm reported earlier [57]. In presence of equimolar amounts of EB, the mean hydrodynamic diameter shifts to 8.13 nm. Upon addition of twelve times molar excess of EB, the mean octamer diameter becomes 7.02 nm. In case of PI, equimolar amounts of PI and DNA gives rise to a hydrodynamic diameter of 6.5 nm, which remains constant even in presence of twelve times molar excess of PI. In either case, the minimum particle size measured corresponds to an intact octamer (within experimental error limits). The observations remain unchanged when the experiments are repeated with HeLa core octamer. Hence EB or PI binding to histone octamer does not lead to its structural disintegration. The circular dichroism spectrum of 3 μM histone octamer remains practically unchanged even in presence of 12 times excess of EB (Fig. S5). The results indicate that EB does not cause any secondary structure perturbation of the histone proteins of the octamer. In the above set of experiments we have shown that the DNA intercalators, PI and EB, interact with core histones. This interaction could potentially alter post-translational modification of core histones, such as acetylation as had been reported in case of mitoxantrone [10] and was therefore explored *ex vivo*. Significantly, PI and EB could alter global acetylation status of histone H3 and H4. More specifically, we have found an alteration in H3K9Ac, H4K5Ac and H4K8Ac upon treatment with PI and EB in a concentration dependent manner (Fig. 3). The extent of ligand-induced alteration of acetylation levels has been quantified (Fig. 3d). PI turns out to be a more potent inhibitor of these acetylation marks *ex vivo*. The extent of repression of H3K9Ac level in HeLa cells in presence of 8 μM PI and EB is 100- and 54-fold respectively. Upon treatment with 8 μM of the ligands, similar trends are observed in case of H4K5Ac (144-fold for PI and 71-fold for EB) and H4K8Ac (85-fold for PI and 57-fold for EB). The concentration of these ligands used in *our ex vivo* studies are in a non-cytotoxic range, as verified by MTT assay (Supplementary Fig. S7). The acetylation status of H3K14 did not show a significant alteration upon PI/EB treatment (Fig. 3a). We have subsequently investigated the alteration of histone H3K9 acetylation status in a purified system using HAT assay. H3K9Ac was altered *in vitro* in presence of the ligands (Fig. 3c), indicating that even in absence of DNA, EB and PI have the potential to alter specific epigenetic signatures. The extent of ligand-induced repression of H3K9Ac level is comparable *in vitro* (Fig. 3d).

4. Discussion

The association of small DNA binding molecules with chromatin needs to be re-examined from the perspective that they might bind to histone also, the integral component of the genetic machinery. Here we have examined in depth the binding potential of classical intercalator, EB and its structural analogue, PI to chromatin and the resultant alteration in structure. The study reports the association and the binding energetics of the intercalators with chromatin, chromatosome, chromosomal DNA and core histones. These ligands induce chromatin compaction and DNA release at the chromatosome level. However, the major and most novel outcome from our current report is the interactions with core histones that has not been previously considered but which likely contribute significantly to evaluate the overall effects of the ligands.

For thermodynamic analysis of the interaction of PI and EB with chromatin, the system has been divided into three components: chromatin, chromatosome, and chromosomal DNA. A similar approach was adopted earlier to study the thermodynamics of the interaction of the groove binder, distamycin [42] and intercalator, sanguinarine with chromatin [7]. ITC shows that EB and PI bind to chromatin and its components with different site sizes. This has been ascribed to presence of double charge and longer length of PI. They bind to chromatosome with lower affinity than chromatin. This trend is consistent with an earlier report whereby EB was shown to bind preferentially to the linker segment compared to the nucleosome [32]. Binding to chromatin, chromatosome and chromosomal DNA are all enthalpy driven. The intercalation of PI/EB into DNA base pairs results in enthalpically favoured van der Waal's stacking. The stacking interaction via intercalation into the base pairs of DNA appears to be the predominant factor for the favourable free energy change. Enthalpy-entropy compensation results in comparable free energy of binding of the ligands with chromatin components. ITC profiles for the binding of PI and EB with monoucleosome reconstituted on a 200 bp DNA containing the 601 nucleosome positioning sequence in the centre [47] (Supplementary Fig. S6) are similar to the thermograms obtained for their association with chromatosome isolated from biological sources suggesting the specificity of the interaction. The binding energetics is also similar in case of reconstituted nucleosome thereby doing away with the possibility of any artefact from the possible presence of other non-histone proteins and RNA in the samples isolated from the cells. At the chromatosome level, binding of EB and PI leads to disruption of the chromatosome structure. Ligand to DNA base ratio of 0.05 is sufficient to observe a DNA release from chromatosomes. It agrees with a previous report [56] which shows that binding of EB to chicken erythrocyte nucleosome core particles results in a step-wise dissociation of the structure. A similar effect on chromatosomes shows that EB is capable of removing linker histones that clamp the DNA in chromatosomes [25]. We checked the absence of DNA release in all calorimetric studies with chromatosomes. Since EB binding to free DNA causes unwinding of the helix [14], changes in sugar pucker, glycosidic torsional angle and phosphodiester torsional angles [15,58,59], the observed effects seem feasible in the chromatin context. It was proposed earlier that intercalation of EB within nucleosomal DNA causes stiffening of the helix. It in turn prohibits bending around the histone octamer, and causes dissociation of nucleosome core particles [56]. Similar explanations may be valid for chromatosomes as well.

The most significant part of our results shows that, EB and PI bind to core histones as well. It contradicts previous literature report [60]. Histone–EB interactions were suggested in some earlier literature reports [53,54] without much emphasis on this observation. Hydrophobic interactions between EB and histone octamer were considered insignificant on the ground that they contributed very little to EB-core particle interaction and that DNA intercalation form the major mode of EB-nucleosomal core particle interaction [54]. In our present report, steady state fluorescence measurements reveal the binding interactions between the ligands and the core octamer. The nature of binding to core octamer influences the quantum yield of fluorescence of the two ligands upon binding. The positively charged ligands may interact with the negatively charged surface of the octamer or occupy the hydrophobic cavity. There are reports [61,62] which suggest that

neutralization of negative charge on nucleosome surface may result in chromatin condensation or folding. It is possible that these positively charged ligands interact with the acidic patch on the face of nucleosome and induce chromatin compaction. DLS data also indicate chromatin compaction. With increase in ligand input concentration, there is a decrease in the intensity weighted mean hydrodynamic diameter or Z_{av} diameter of the ensemble of particles in the measurement window. An interesting observation in this regard is the decrease in polydispersity index with increase in the concentration of EB and PI concentration. Polydispersity, which is defined as the ratio of weight average and number average molecular weights, gives an idea of the molecular weight distribution. It is extrapolated to obtain an idea about the particle size distribution. In case of association of EB and PI with chromatin, the decrease in polydispersity index indicates that upon ligand binding, particles of chromatin adopt a structure that is more homogeneous than untreated chromatin. In this context, it is relevant to correlate chromatin compaction with ligand induced repression of histone acetylation. Histone acetylation in general opens up chromatin structure and leads to gene activation [63] barring a few exceptions [64]. In the present report, small molecule induced structural alteration of chromatin promoting hypoacetylation of histones could be a novel mechanism to regulate chromatin function [10]. In addition to explanation given earlier, the ability of the ligand(s) to interact with both the DNA and histone components leads to disintegrate chromatosome structure causing DNA release.

The binding affinity of EB and PI for core histones is comparable to chromosomal DNA. This is manifested in the ITC results for the binding of chromatin and chromatosome with EB and PI. Biphasic transition is not observed in the thermograms and best fit of the calorimetric data for these two systems was obtained using "one set of binding site" model even though EB and PI have two interacting partners. The entropy driven nature of the interaction of EB and PI with core histones in contrast to enthalpy driven nature of the association of the DNA–protein complexes like chromatin and chromatosome suggest the roles of release of bound water in favouring the negative free energy change in case of association of EB and PI with core histones.

To sum up, this report highlights the dual binding property of two classical DNA intercalators, EB and PI in the chromatin context. The histone binding property of EB and PI adds a layer of complexity to EB/PI–chromatin interaction. We have observed a ligand induced alteration of global acetylation status of histone H3 (K9Ac) and H4 (K5Ac and K8Ac) in HeLa cells. Further, *in vitro* HAT assay has also established ligand induced alteration of histone acetylation (H3K9Ac) in absence of DNA. Keeping in mind, the histone binding ability of these classical DNA-binding ligands, experiments employing EB and PI as cellular probes might preferably be accompanied with appropriate control.

Acknowledgements

We acknowledge with profound respect Late Professor Jonathan Widom, Northwestern University, for his kind gift of the 601 positioning sequence. We thank the animal house facility of the Bose Institute, Kolkata for the supply of Sprague–Dawley rat liver. We thank Professor Abhijit Chakrabarti for his permission to use the CD facility of Biophysics & Structural Genomics Division of SINP. We thank Ms. Saptaparni Ghosh for her help in the preparation of graphical abstract. This work was supported by intramural grants from the Molecular Mechanism of Disease and Drug Action (MMDDA) project (Grant 11-R&D-SIN-5.04) and Biomolecular Assembly, Recognition and Dynamics (BARD) project (Grant 12-R&D-SIN-5.04−0103) from the Department of Atomic Energy (DAE), Government of India. CD acknowledges the Ramalingaswami Fellowship.

Appendix A. Supplementary data

Supplementary data associated with this article can be found, in the online version, at http://dx.doi.org/10.1016/j.fob.2014.02.006.

References

[1] Kornberg, R.D. (1977) Structure of chromatin. Annu. Rev. Biochem. 46, 931–954.
[2] McGhee, J.D. and Felsenfeld, G. (1980) Nucleosome structure. Annu. Rev. Biochem. 49, 1115–1156.
[3] Luger, K., Mader, A.W., Richmond, R.K., Sargent, D.F. and Richmond, T.J. (1997) Crystal structure of the nucleosome core particle at 2.8 A resolution. Nature 389, 251–260.
[4] Hurley, L.H. (2002) DNA and its associated processes as targets for cancer therapy. Nat. Rev. Cancer 2, 188–200.
[5] Ghosh, S., Majumder, P., Pradhan, S.K. and Dasgupta, D. (2010) Mechanism of interaction of small transcription inhibitors with DNA in the context of chromatin and telomere. Biochim. Biophys. Acta 1799, 795–809.
[6] Dasgupta, D., Majumder, P. and Banerjee, A. (2012) A revisit of the mode of interaction of small transcription inhibitor with genomic DNA. J. Biosci. 37, 475–481.
[7] Selvi, B.R., Pradhan, S.K., Shandilya, J., Das, C., Sailaja, B.S., Shankar, G.N., Gadad, S.S., Reddy, A., Dasgupta, D. and Kundu, T.K. (2009) Sanguinarine interacts with chromatin, modulates epigenetic modifications, and transcription in the context of chromatin. Chem. Biol. 16, 203–216.
[8] Rabbani, A., Finn, R.M., Thambirajah, A.A. and Ausio, J. (2004) Binding of antitumor antibiotic daunomycin to histones in chromatin and in solution. Biochemistry 43, 16497–16504.
[9] Hajihassan, Z. and Rabbani-Chadegani, A. (2011) Interaction of mitoxantrone, as an anticancer drug, with chromatin proteins, core histones and H1, in solution. Int. J. Biol. Macromol. 48, 87–92.
[10] Khan, S.N., Yennamalli, R., Subbarao, N. and Khan, A.U. (2011) Mitoxantrone induced impediment of histone acetylation and structural flexibility of the protein. Cell Biochem. Biophys. 60, 209–218.
[11] Fuller, W. and Waring, M. (1964) A molecular model for the interaction of ethidium bromide with deoxyribonucleic acid. Berichte der Bunsengesellschaft fÃ¼r physikalische. Chemie 68, 805–808.
[12] Lerman, L. (1961) Structural considerations in the interaction of DNA and acridines. J. Mol. Biol. 3, 18–30.
[13] Jones, R.L., Lanier, A.C., Keel, R.A. and Wilson, W.D. (1980) The effect of ionic strength on DNA-tigand unwinding angles for acridine and quinoline derivatives. Nucleic Acids Res. 8, 1613.
[14] Wang, J.C. (1974) The degree of unwinding of the DNA helix by ethidium. I. Titration of twisted PM2 DNA molecules in alkaline cesium chloride density gradients. J. Mol. Biol. 89, 783–801.
[15] Sobell, H.M., Tsai, C.C., Jain, S.C. and Gilbert, S.G. (1977) Visualization of drug-nucleic acid interactions at atomic resolution. III. Unifying structural concepts in understanding drug–DNA interactions and their broader implications in understanding protein–DNA interactions. J. Mol. Biol. 114, 333–365.
[16] Angerer, L.M., Georghiou, S. and Moudrianakis, E.N. (1974) Studies on the structure of deoxyribonucleoproteins. Spectroscopic characterization of the ethidium bromide binding sites. Biochemistry 13, 1075–1082.
[17] Lurquin, P.F. (1974) The use of intercalating dye molecules in the study of chromatin structure. Chem. Biol. Interact. 8, 303–312.
[18] Lurquin, P.F. and Seligy, V.L. (1972) Binding of ethidium bromide to avian erythrocyte chromatin. Biochem. Biophys. Res. Commun. 46, 1399–1404.
[19] Lawrence, J.J., Chan, D.C. and Piette, L.H. (1976) Conformational state of DNA in chromatin subunits. Circular dichroism, melting, and ethidium bromide binding analysis. Nucleic Acids Res. 3, 2879–2893.
[20] Lawrence, J.J. and Daune, M. (1976) Ethidium bromide as a probe of conformational heterogeneity of DNA in chromatin. The role of histone H1. Biochemistry 15, 3301–3307.
[21] Lawrence, J.J. and Louis, M. (1974) Ethidium bromide as a probe of chromatin structure. FEBS Lett. 40, 9–12.
[22] Paoletti, J., Magee, B.B. and Magee, P.T. (1977) The structure of chromatin: interaction of ethidium bromide with native and denatured chromatin. Biochemistry 16, 351–357.
[23] LaRue, H. and Pallotta, D. (1976) A study of the interaction between ethidium bromide and rye chromatin: comparison with calf thymus chromatin. Nucleic Acids Res. 3, 2193–2206.
[24] Doenecke, D. (1976) Binding of ethidium bromide to fractionated chromatin. Exp. Cell Res. 100, 223–227.
[25] Fenske, H., Eichhorn, I., Bottger, M. and Lindigkeit, R. (1975) Evidence of altered histone interactions, as investigated by removal of histones, in chromatin isolated from rat liver nuclei by a conventional method. Nucleic Acids Res. 2, 1975–1985.
[26] Stratling, W.H. and Seidel, I. (1976) Relaxation of chromatin structure by ethidium bromide binding: determined by viscometry and histone dissociation studies. Biochemistry 15, 4803–4809.

[27] Benyajati, C. and Worcel, A. (1976) Isolation, characterization, and structure of the folded interphase genome of *Drosophila melanogaster*. Cell 9, 393–407.
[28] Doenecke, D. (1977) Ethidium bromide (EB) binding to nucleosomal DNA. Effects on DNA cleavage patterns. Exp. Cell Res. 109, 309–315.
[29] Paoletti, J. (1978) Relaxation of chromatin structure induced by ethidium binding: 1–micrococcal nuclease digestion of the ethidium–chromatin complex. Biochem. Biophys. Res. Commun. 81, 193–198.
[30] Barni, S. and Gerzeli, G. (1982) Ultrastructure and fluorescence of chromatin: interaction of propidium iodide with DNA after different pretreatments. Cell Biol. Int. Rep. 6, 544.
[31] Taquet, A., Labarbe, R. and Houssier, C. (1998) Calorimetric investigation of ethidium and netropsin binding to chicken erythrocyte chromatin. Biochemistry 37, 9119–9126.
[32] Cartwright, I.L., Hertzberg, R.P., Dervan, P.B. and Elgin, S. (1983) Cleavage of chromatin with methidiumpropyl-EDTA. Iron (II). Proc. Natl. Acad. Sci. 80, 3213.
[33] Erard, M., Das, G.C., de Murcia, G., Mazen, A., Pouyet, J., Champagne, M. and Daune, M. (1979) Ethidium bromide binding to core particle: comparison with native chromatin. Nucleic Acids Res. 6, 3231–3253.
[34] Hurley, I., Osei-Gyimah, P., Archer, S., Scholes, C.P. and Lerman, L.S. (1982) Torsional motion and elasticity of the deoxyribonucleic acid double helix and its nucleosomal complexes. Biochemistry 21, 4999–5009.
[35] Wang, J., Hogan, M. and Austin, R. (1982) DNA motions in the nucleosome core particle. Proc. Natl. Acad. Sci. USA 79, 5896.
[36] Benezra, R., Cantor, C.R. and Axel, R. (1986) Nucleosomes are phased along the mouse beta-major globin gene in erythroid and nonerythroid cells. Cell 44, 697–704.
[37] Sinden, R.R., Carlson, J.O. and Pettijohn, D.E. (1980) Torsional tension in the DNA double helix measured with trimethylpsoralen in living *E. coli* cells: analogous measurements in insect and human cells. Cell 21, 773–783.
[38] Pettijohn, D.E. and Pfenninger, O. (1980) Supercoils in prokaryotic DNA restrained in vivo. Proc. Natl. Acad. Sci. USA 77, 1331–1335.
[39] Ren, J., Jenkins, T.C. and Chaires, J.B. (2000) Energetics of DNA intercalation reactions. Biochemistry 39, 8439–8447.
[40] Giangare, M.C., Prosperi, E., Pedrali-Noy, G. and Bottiroli, G. (1989) Flow cytometric evaluation of DNA stainability with propidium iodide after histone H1 extraction. Cytometry 10, 726–730.
[41] Schroter, H., Maier, G., Ponstingl, H. and Nordheim, A. (1985) DNA intercalators induce specific release of HMG 14, HMG 17 and other DNA-binding proteins from chicken erythrocyte chromatin. EMBO J. 4, 3867–3872.
[42] Majumder, P. and Dasgupta, D. (2011) Effect of DNA groove binder distamycin A upon chromatin structure. PLoS One 6, e26486.
[43] Waring, M.J. (1965) Complex formation between ethidium bromide and nucleic acids. J. Mol. Biol. 13, 269–282.
[44] Rentzeperis, D., Medero, M. and Marky, L.A. (1995) Thermodynamic investigation of the association of ethidium, propidium and bis-ethidium to DNA hairpins. Bioorg. Med. Chem. 3, 751–759.
[45] Das, C., Hizume, K., Batta, K., Kumar, B.R., Gadad, S.S., Ganguly, S., Lorain, S., Verreault, A., Sadhale, P.P., Takeyasu, K. and Kundu, T.K. (2006) Transcriptional coactivator PC4, a chromatin-associated protein, induces chromatin condensation. Mol. Cell Biol. 26, 8303–8315.
[46] Blobel, G. and Potter, V.R. (1966) Nuclei from rat liver: isolation method that combines purity with high yield. Science 154, 1662–1665.
[47] Kundu, T.K., Wang, Z. and Roeder, R.G. (1999) Human TFIIIC relieves chromatin-mediated repression of RNA polymerase III transcription and contains an intrinsic histone acetyltransferase activity. Mol. Cell Biol. 19, 1605–1615.
[48] Chakrabarti, S., Roy, P. and Dasgupta, D. (1998) Interaction of the antitumor antibiotic chromomycin A< sub> 3</sub> with glutathione, a sulfhydryl agent, and the effect upon its DNA binding properties. Biochem. Pharmacol. 56, 1471–1479.
[49] Mir, M.A. and Dasgupta, D. (2001) Interaction of antitumor drug, mithramycin, with chromatin. Biochem. Biophys. Res. Commun. 280, 68–74.
[50] Sinha, M., Ghose, J. and Bhattarcharyya, N.P. (2011) Micro RNA, -214,-150, -146a and-125b target Huntingtin gene. RNA Biol. 8, 1005–1021.
[51] Haq, I., Ladbury, J.E., Chowdhry, B.Z., Jenkins, T.C. and Chaires, J.B. (1997) Specific binding of hoechst 33258 to the d(CGCAAATTTGCG)2 duplex: calorimetric and spectroscopic studies. J. Mol. Biol. 271, 244–257.
[52] Haq, I. (2002) Thermodynamics of drug-DNA interactions. Arch. Biochem. Biophys. 403, 1–15.
[53] McMurray, C.T. and van Holde, K.E. (1991) Binding of ethidium to the nucleosome core particle. 1. Binding and dissociation reactions. Biochemistry 30, 5631–5643.
[54] McMurray, C.T., Small, E.W. and van Holde, K.E. (1991) Binding of ethidium to the nucleosome core particle. 2. Internal and external binding modes. Biochemistry 30, 5644–5652.
[55] Chou, W.Y., Marky, L.A., Zaunczkowski, D. and Breslauer, K.J. (1987) The thermodynamics of drug–DNA interactions: ethidium bromide and propidium iodide. J. Biomol. Struct. Dyn. 5, 345–359.
[56] McMurray, C.T. and van Holde, K.E. (1986) Binding of ethidium bromide causes dissociation of the nucleosome core particle. Proc. Natl. Acad. Sci. USA 83, 8472–8476.
[57] Feng, H.P., Scherl, D.S. and Widom, J. (1993) Lifetime of the histone octamer studied by continuous-flow quasielastic light scattering: test of a model for nucleosome transcription. Biochemistry 32, 7824–7831.
[58] Jain, S.C., Tsai, C.C. and Sobell, H.M. (1977) Visualization of drug-nucleic acid interactions at atomic resolution. II. Structure of an ethidium/dinucleoside monophosphate crystalline complex, ethidium:5-iodocytidylyl (3′–5′) guanosine. J. Mol. Biol. 114, 317–331.
[59] Tsai, C.C., Jain, S.C. and Sobell, H.M. (1977) Visualization of drug-nucleic acid interactions at atomic resolution. I. Structure of an ethidium/dinucleoside monophosphate crystalline complex, ethidium:5-iodouridylyl (3′–5′) adenosine. J. Mol. Biol. 114, 301–315.
[60] Chitre, A.V. and Korgaonkar, K.S. (1979) Binding of ethidium bromide and quinacrine hydrochloride to nucleic acids and reconstituted nucleohistones. Biochem. J. 179, 213–219.
[61] Baker, A.M., Fu, Q., Hayward, W., Lindsay, S.M. and Fletcher, T.M. (2009) The Myb/SANT domain of the telomere-binding protein TRF2 alters chromatin structure. Nucleic Acids Res. 37, 5019–5031.
[62] Baker, A.M., Fu, Q., Hayward, W., Victoria, S., Pedroso, I.M., Lindsay, S.M. and Fletcher, T.M. (2011) The telomere binding protein TRF2 induces chromatin compaction. PLoS One 6, e19124.
[63] Kundu, T.K., Palhan, V.B., Wang, Z., An, W., Cole, P.A. and Roeder, R.G. (2000) Activator-dependent transcription from chromatin in vitro involving targeted histone acetylation by p300. Mol. Cell 6, 551–561.
[64] Strahl, B.D. and Allis, C.D. (2000) The language of covalent histone modifications. Nature 403, 41–45.